JOURNAL OF THE BALKAN GEOPHYSICAL SOCIETY, Vol. 1, No 1, February 1998, p. 3-13, 8 figs.

A smoothness constrained algorithm for the fast 2-D inversion of DC resistivity and induced polarization data

P.I. Tsourlos[*], J.E. Szymanski[**] and G.N. Tsokas[*]

[*]Geophysical Laboratory, Aristotelian University of Thessaloniki, 54006 Thessaloniki Greece.
[**]Department of Electronics, University of York, Heslington, York Y01 5DD, U.K.

(Received 10 January 1998; accepted 1 February 1998)

Abstract: *A fast smoothness constrained algorithm for the 2-D inversion of direct current and induced polarization data is presented. The procedure is fully automated and accelerated by the use of a Quasi-Newton update of the Jacobian matrix. The need for a fast algorithm is discussed and a detailed presentation of its features is given. The features of the algorithm are presented in detail and comparisons to other techniques are shown. The algorithm is also used to invert Induced Polarization (IP) data sets. Finally, tests of the algorithm with synthetic and real data are presented. The algorithm proves to be robust noise insensitive and produces good quality inversions. The tests with real data indicated that it could be a reliable tool for data interpretation.*

Key Words: *Resistivity Inversion, IP Inversion, Smoothness Constrained*

INTRODUCTION

Electrical resistivity and induced polarization techniques are used to a wide range of geophysical problems. Among the existing measuring modes 2-D resistivity/IP prospecting can give information about both the lateral and vertical variations of the earth's properties and can be used in a qualitative fashion for the identification of the structure and depth of buried features.

The potential use of 2-D prospecting is of considerable current interest due to the development of automatically multiplexed measuring systems which facilitate the acquisition of a large number of measurements in a limited time (Noel and Walker 1991; Dahlin, 1993). However, it is essential to develop reliable and robust interpretation-inversion algorithms, which are able to produce a “deblurred” subsurface image in order to render the information accessible to non-experts.

The traditional methods of data interpretation, such as the construction of a pseudosection (Edwards, 1977) provide only a rather qualitative insight into the region of interest and can only cope with the traditional (surface linear-arrays, set range of spacings) measuring schemes. Other interpretation techniques such as an operator-controlled data fitting technique (eg. Stretenovic and Marcetic, 1992) are inadequate for interpreting large data sets. Approximate techniques such as the back-projection technique (Noel and Walker, 1991) can produce artefacts and their results are still not easily accessible to non-experts.

The advent of fast computers allowed the development of the resistivity and IP inversion schemes, which aim to construct an estimate of a subsurface resistivity distribution, which is consistent with the experimental data. This is a fully non-linear procedure and its "accurate" treatment involves iterative full-matrix inversion algorithms, which can give good quality results. The inversion of earth resistivity and IP data is an ill-conditioned problem because large variations in physically defined parameters may result into small variations in the observed data that make the inversion algorithm unstable. Additionally, factors such as the noise contamination of the data and an inappropriate choice of the parametrized blocks can further increase this instability.

Several non-linear resistivity and IP inversion algorithms which can handle ill-conditioning have been reported in literature mainly based on the damped least-squares that is also known as the Levenberg-Marquadt method (Trip et al., 1984; Smith

and Vozoff, 1984; Pelton et al., 1978). The Levenberg-Marquadt method can produce very good results but spurious noise-related artifacts can appear in the case of noisy data. Further, the produced results will be highly dependent on the ``accidental" (successful or not) choice of the initial model (Constable et al., 1987).

One other way to tackle the instability of the inverse problem is to impose a smoothness constraint. The technique has been proposed for the geophysical case by Constable et al. (1987) who named it Occam inversion (due to the 14th century philosopher) and they applied it to the 1-D resistivity and magneto-telluric inverse problems. The smoothness constraint inversion will produce a simplified model which is a reasonable representation of the subsurface and at the same time guarantees the inversion stability and most importantly produces a model which is based on the characteristic that the user has chosen (namely the pattern of the smoothness) and not on some arbitrary initial guess. Smoothness constrained algorithms for the 2-D earth resistivity case have been presented by Sasaki (1989, 1992), Xu (1993), Elis and Oldenburg (1994). Further, Oldenburg and Li (1994) presented schemes that imposed smoothness constrain to the inversion of IP data.

The advent of automatically controlled instrumentation increased the amount of the collected measurements and the speed of the data collection. A rapid initial interpretation of these data sets is valuable and will help to check if the right survey settings are chosen. Traditionally, the “approximate” inversion techniques are used for this purpose whilst “accurate” techniques are usually used for final processing/ interpretation after the survey has finished.

For these reasons, it is clear that there is a scope for a fast fully non-linear algorithm, which could cope with the increased amount of data and could be used as a tool for more accurate initial data interpretation. For most of the iterative inversion schemes and for a typical data set (eg.. 40 electrodes, 300 measurements) the calculation of the Jacobian matrix takes approximately 70% of the iteration time thus the inversion procedure can be accelerated significantly by avoiding the direct calculation of the Jacobian at every iteration. This can be achieved by the use of the Quasi-Newton techniques.

This paper involves the presentation of a Quasi-Newton smoothness constrained inversion scheme for the 2-D inversion of earth resistivity and IP data, which is based on the work of Tsourlos (1995). Loke and Barker (1996) have developed a similar algorithm independently for the resistivity case. A proven 2.5-D Finite Element Method (FEM) scheme was used as the platform for the forward resistivity calculations (Tsourlos, 1995). The adjoint equation approach (McGillivray and Oldenburg, 1990) was incorporated into the FEM scheme in order to calculate the Jacobian matrix J (the divergence of the observations in respect of changes of the model's resistivity) when necessary.

QUASI-NEWTON TECHNIQUES

Quasi-Newton (QN) (or variable metric) techniques are a class of non-linear optimization methods which seek to approximate the Jacobian at each iteration instead of calculating it from scratch. This type of method is similar to the Gauss-Newton technique except that the Jacobian matrix **J** is approximated by a matrix **B** which is corrected and updated from iteration to iteration (Fletcher, 1987). Use of the QN techniques in the 2-D resistivity inverse problem has been reported by Shima (1990) who used Powell's algorithm (Powell, 1970). Further, Loke and Barker (1996) presented a QN technique within a smoothness constrained algorithm.

Consider a measurement vector y and an initial property distribution vector xo. If $\mathbf{J_o}$ is the Jacobian matrix and $\mathbf{F(x_o)}$ is the forward modelling response then one iteration of any optimization technique which involves matrix inversion will produce a parameter correction vector $\mathbf{dx_o}$. The forward response for the new estimate will be $\mathbf{F(x_o + dx_o)}$. The target is to find an approximate expression $\mathbf{B_1}$ of the Jacobian $\mathbf{J_1}$ for the new iteration without calculating it from scratch. Broyden (1965) showed that the unique $\mathbf{B_1}$ can be defined as:

$$\mathbf{B_1 = J_o - \{J_o dx_o - [F(x_o)-F(x_1)]\}dx_o / (dx_o^T dx_o)} \quad (1)$$

Equation (1) can be generalized to update the estimate of the Jacobian in every iteration. For the k+1 iteration the approximate estimate is given by:

$$\mathbf{B_{k+1} = B_k - \{B_k dx_k - [F(x_k) - F(x_{k+1})]\}dx_k / (dx_k^T dx_k)} \quad (2)$$

One of the disadvantages of the QN methods is that they have superlinear convergence, as opposed to the quadratic convergence of the Newton-like methods. In 2-D resistivity inversion QN techniques typically result in an average increase of 1-3 iterations. For most cases, however, this trade-off leads to less computational time although the number of iterations increases. Only in cases when the iteration time is dominated by the matrix inversion (extremely large data sets) does this become a real disadvantage.

The main disadvantage of the technique is that it is subject to errors involved with the finite difference type of approximation of equation (2). One problem is that round-off errors propagate: each new approximate Jacobian is a function of the previous (also approximate) Jacobian. This is an extra source of error in the inversion (additional to the observation errors) and might cause instability. It will be shown that was not found to be the case: the smoothness constraint in the inversion scheme prevented the technique from causing unstable solutions.

ALGORITHM DESCRIPTION

During the 2-D resistivity reconstruction procedure, the subsurface is considered, as a set of individual blocks that have intrinsic resistivity parameters subject to the independent adjusment while the size of the blocks kept constant. The aim is to calculate a subsurface resistivity estimate **x** for which the difference **dy** between the observed data **y** and the modelled data **F(x)** (calculated using the forward modelling technique) is minimized

Since we are dealing with a non-linear problem this procedure has to be iterative: In every iteration, an improved resistivity estimate is sought and eventually the procedure stops until certain convergence criteria are met (i.e. until the RMS error is practically stable). An Occam's inversion scheme was applied in order to produce a stable non-linear algorithm for the 2-D inversion of earth resistivity data. A general description of the algorithm follows.

Initial Steps

Given a measured data set **y**

- Define the model parameters.
- Produce the matrix C that describes the smoothness pattern of the model.
- Define an initial resistivity estimate $\mathbf{x_o}$ and calculate the model response $\mathbf{f(x_0)}$.
- Calculate the Jacobian matrix $\mathbf{J_0}$ which corresponds to $\mathbf{x_o}$ using the adjoint equation approach and set $\mathbf{B_0}=\mathbf{J_0}$.
- Set the initial value λ_0 of the Lagranian multiplier.
- Set the inversion stopping criteria: slow convergence rate (practically stable RMS error) or divergence.

1. At the k_{th} iteration the resistivity correction vector $d\mathbf{x_k}$ is given by

$$d\mathbf{x_k} = (\mathbf{B_k}^T \mathbf{B_k} + (\mathbf{C}^T \mathbf{C})^{-1} \mathbf{B_k}^T \mathbf{dy_k} \quad (3)$$

where $\mathbf{B_k}$ is the Quasi-Newton Jacobian estimate which corresponds to the $\mathbf{x_k}$ resistivity distribution, and $\mathbf{dy_k} = \mathbf{y}\text{-}\mathbf{F}(\mathbf{x_k})$.

2. Set the new resistivity estimate $\mathbf{x_{k+1}} = \mathbf{x_k} + d\mathbf{x_k}$ and calculate the forward response of the new model $\mathbf{F}(\mathbf{x_{k+1}})$.

3. If one of the stopping criteria are met then terminate the procedure else find the new QN estimate of the Jacobian matrix using equation (3) and go to step 1.

A simplified flow-chart of the QN Occam algorithm is shown in Figure 1.

Inversion of the IP data

The IP effect can be described by a macroscopic physical parameter called chargeability m that is a unitless parameter confined to be in the range zero and unity (Siegel, 1959). If **x** shows the intrinsic resistivities of the subsurface then the observed apparent resistivities can be expressed as **d=F(x)** where **F** is the forward modelling operator. Similarly, the effect of the intrinsic chargeabilities can be expressed as $\mathbf{d_m}=\mathbf{F[x(1-m)]}$. Consequently, the inversion of IP data can be related to the inversion of the resistivity data. The apparent chargeability vector $\mathbf{m_a}$ can be expressed as:

$$\mathbf{m_a} = (\mathbf{d_{m-}}\, \mathbf{d})/\, \mathbf{d_m} = (\mathbf{F[x(1-m)]} - \mathbf{F(x)}) / \mathbf{F[x(1-m)]} \quad (4)$$

assuming that $\mathbf{F^{-1}}$ expresses the inverse operator the chargeability can be expressed as (Oldenburg and Li, 1994):

$$\mathbf{m} = (\mathbf{F^{-1}[x(1-m)]} - \mathbf{F^{-1}(x)}) / \mathbf{F^{-1}[x(1-m)]} \quad (5)$$

In other words the subsurface chargeability can be obtained by equation 5 after performing two inversions (using the described algorithm and identical inversion parameters) on the data sets obtained from the resistivity and the IP survey.

PRACTICAL CONSIDERATIONS

The smoothness matrix **C** describes the smoothness relations between the parameters. The smoothness pattern used in this algorithm is given by

$$d\mathbf{x}_j = [\, a_j^x (dx_j^E + dx_j^W) + a_j^z (dx_j^N + dx_j^S) - 2 (a_j^x + a_j^z) dx_j \,] \quad (6)$$

where $d\mathbf{x}_j$ is the smoothness of the jth block, E,W,N,S indicate its four immediate neighbors, a_j^x and a_j^z are weighting factors which control the roughness in the horizontal and vertical direction respectively. They are adjusted in such a way that they compensate for the possible unequal length dx_j , and thickness dz_j of the parameter j as suggested by deGroot and Constable (1990).

In order render the algorithm fully automated, a scheme for automatic generation of the parameter space was included. The parameters are adjusted in a pseudosection-like form: the number of parameters in every layer is symmetrically reduced as depth increases. That is because sensitivity analysis indicated that parameters at the edges tended to become irrelevant as depth increased. The number of the parameter layers is set equal to the max n-separation of the measured data set and the thickness of each layer is set as 0.5 of the inter-electrode spacing for every array used. Each parameter column is positioned between two subsequent electrode positions. In Figure 2a the resultant parameter mesh for the case of 20 electrodes and n-separation of 5 for the dipole-dipole, pole-pole and pole-dipole arrays is depicted. Note also that the x dimension of side and the z dimension of the bottom parameters were set to be quite large (>8 electrode spacings) to simulate infinite boundaries.

Further the option of changing the number of the parameter layers and /or redefine the thicknesses of the existing parameter layers was introduced into the

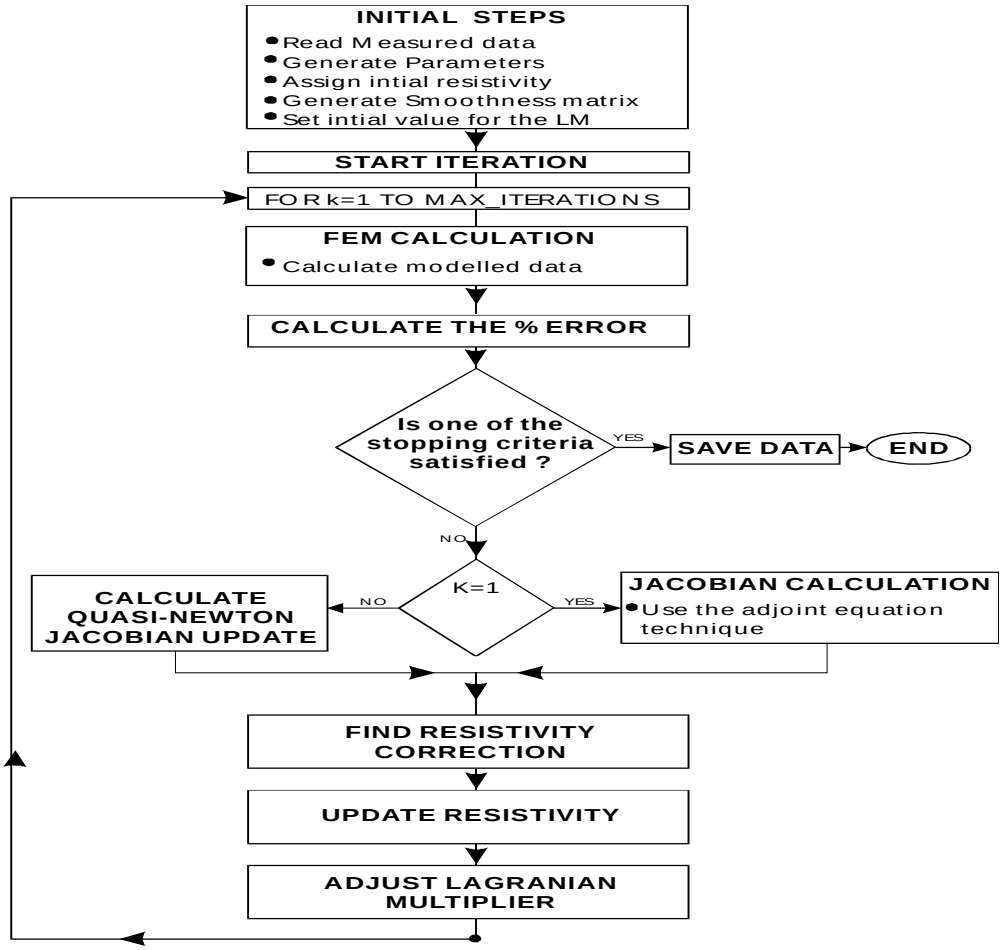

FIG. 1. A simplified flow-chart of the algorithm.

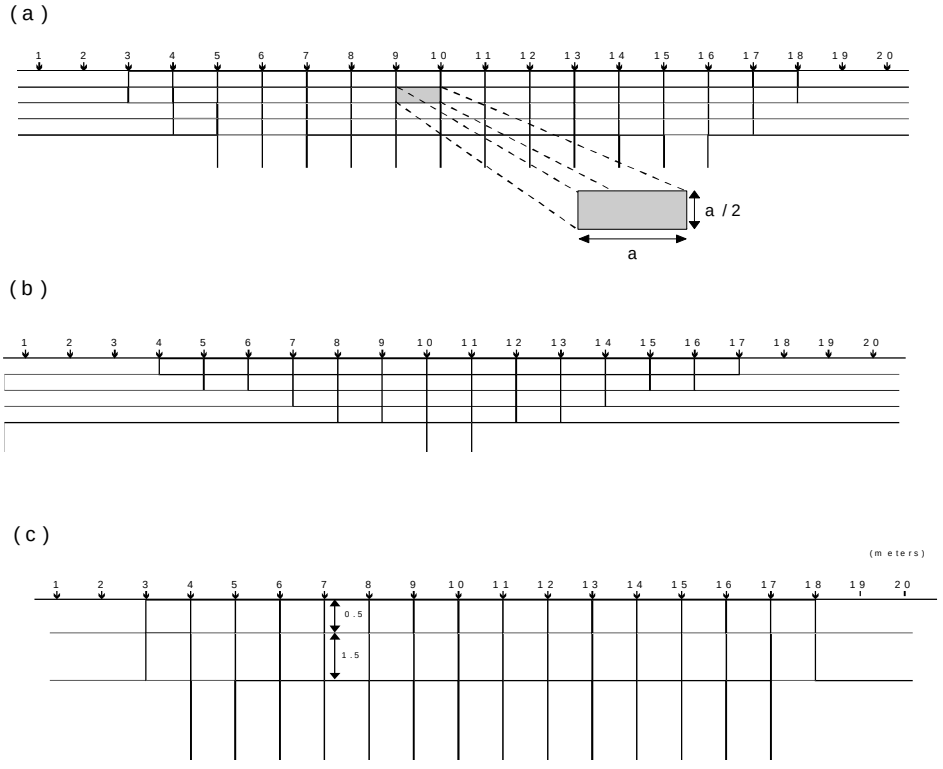

FIG. 2. The parametrization scheme used by the algorithm: a) case of dipole-dipole, pole-pole, pole-dipole arrays (20 electrodes, n=5), b) case of Wenner array (20 electrodes, n=5), c) case of redefined number of layers and thicknesses.

scheme. This was made because in many cases there is reliable prior information concerning the studied area (i.e. prior information about the layer structure in the studied area exists or the targets have known depths). In Figure 2c the case for defining 3 layers with different thicknesses is depicted.

An empirical way for deciding the Lagranian multiplier (LM) at every iteration is used. This scheme was preferred to the 1-D line search procedure (test several LM values and find the optimum LM value by interpolation) since the later proved to be quite time-consuming: a modest line search needs at least three repetitions of the forward modelling and matrix inversion procedure.

The empirical scheme (which was established after several tests with synthetic and real data) is the following:

$\mu_\kappa = \mu_{\kappa-1}/2$ if k< 4 or k=4

$\mu_\kappa = \mu_{\kappa-1}$ if k> 4 κ=1,2,..number of iterations (7)

This scheme proved quite satisfactory and in the tested cases produced inversions very similar to those obtained by the 1-D line search scheme.

APPLICATION AND EVALUATION OF THE ALGORITHM

The described algorithm was applied to a series of synthetic data. The finite element method was used as the forward modelling technique. The Jacobian matrix was calculated by the adjoint equation technique. The matrix inversion was performed by the use of the singular value decomposition routine of Press et al. (1987).

Because of the option of assigning different thicknesses for a parameter layer and since the finite element mesh is created in accordance with the parameter mesh, the initial Jacobian matrix (assuming a homogeneous ground as a starting model) cannot be precalculated and stored as a look-up file. Each parametrization scheme will result in a different initial Jacobian matrix. Thus, despite the use of the QN technique the routine for calculating the Jacobian is included in the scheme. This also gives the flexibility of starting the inversion with any desirable initial model and, most importantly, the option to chose the ``traditional" slower inversion which involves full Jacobian calculations (abandoning the QN technique).

Several comparison tests were made in order to evaluate the performance of the algorithm. In Figure 3 the results of the inversion of the noise-free data of the model of Figure 3a. The inversions with and without the QN Jacobian matrix update can be seen in Figures 3b,c respectively. No significant difference as far as the results are concerned can be observed. Both techniques achieved a similar % RMS error and the only difference lies to the convergence pattern (see Figure 3d).

Similar results were also obtained from the inversion of the dipole-dipole data (5% random noise) from the model of Figure 4a. The inversions with and without the QN Jacobian matrix update can be seen in Figures 4b,c respectively. The convergence pattern of both techniques is depicted in Figure 4d. The advantage that the QN technique has as far as the computational time is concerned can be seen clearly in Figure 5.

Finally, in Figure 6b,c the inversion results of the resistivity and IP dipole-dipole data respectively for the models in Figure 6a are shown. The results indicate that the algorithm successfully reconstructed the highly polarized body.

APPLICATION OF THE ALGORITHM TO REAL DATA

The algorithm produced satisfactory results when synthetic data were considered but it is obvious that conclusive/convincing test for a scheme that is designed for field data interpretation can only be made with real data. Furthermore, these real data should be from sites where there is a good knowledge of the existing targets in order to check/verify the inversion results. This type of inversion examples are presented below:

Drain (University of York)

The data set which was obtained over a drain at the courtyard of the Department of Electronics at the University of York was inverted using the QN Occam inversion. The position of the drain in relation to the measured section is depicted in Figure 7a. The pseudosection of the dipole-dipole data set can be seen in Figure 7b (24 electrodes, dipole length=60 cm, n_{max}=8, 137 measurements).

The inversion after 6 iterations (7.2% RMS error) can be seen in Figure 7c. Despite the 3-D geometry of the target the inverted image delineates the limits of the drain quite accurately - only the top of the drain is somewhat misplaced - and no major artifacts appear.

“Sting” Cave (Williamson County, Texas)

A dipole-dipole data set was measured over a known cave (4T Ranch area-Williamson County, Texas) by Advanced Geosciences Inc. in order to validate their automated resistivity system (Sting/ Swift system). The measured section involves 28 electrodes, 4.5 metres apart and the maximum n-separation was 8 dipoles (171 data-points). The data are shown in a pseudosection form in Figure 8b. The position of the previously known cave in relation to the section is depicted in Figure 8a.

The pseudosection reveals an anomaly situated at

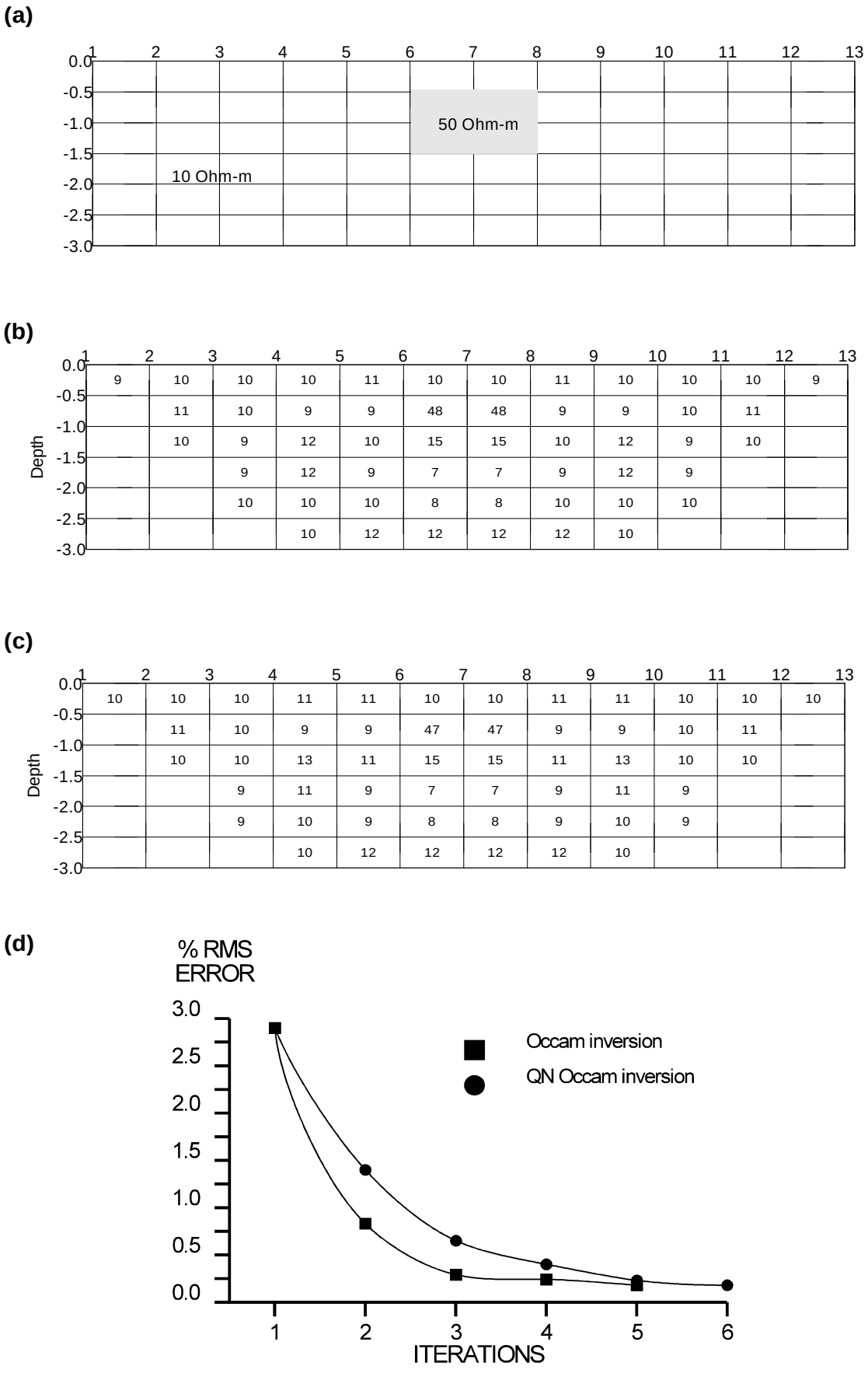

FIG. 3. Inversion of synthetic dipole-dipole data (noise-free, 15 electrodes, n=5): a) the model used to produce the data. b) Inversion results using the QN Occam method. c) Inversion results using the Occam method. d) The convergence of the two techniques.

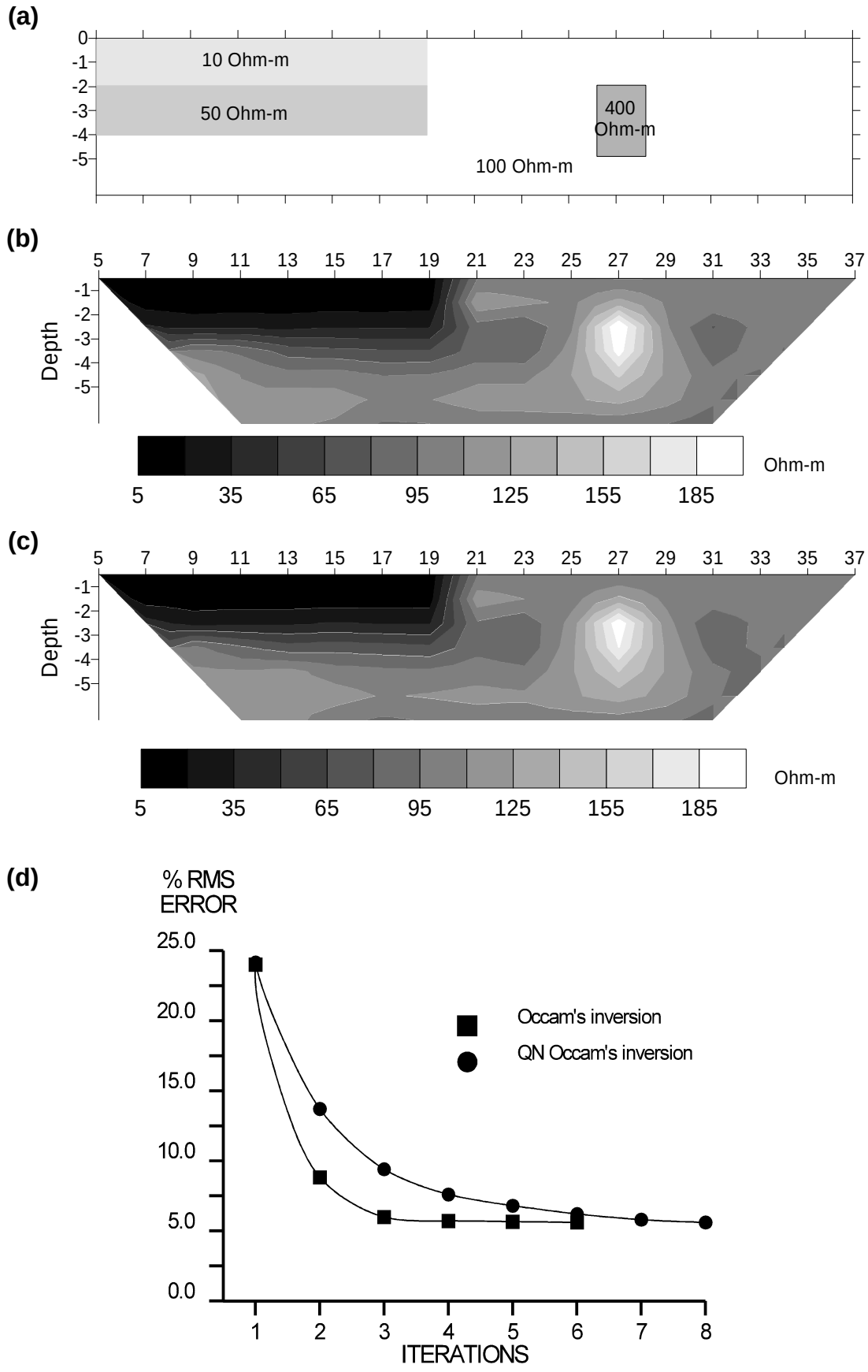

FIG. 4. Inversion of synthetic dipole-dipole data (5% added noise, 20 electrodes, n=6): (a) the model used to produce the data. (b) Inversion results using the QN Occam method. (c)Inversion results using the Occam method. (d) The convergence of the two techniques.

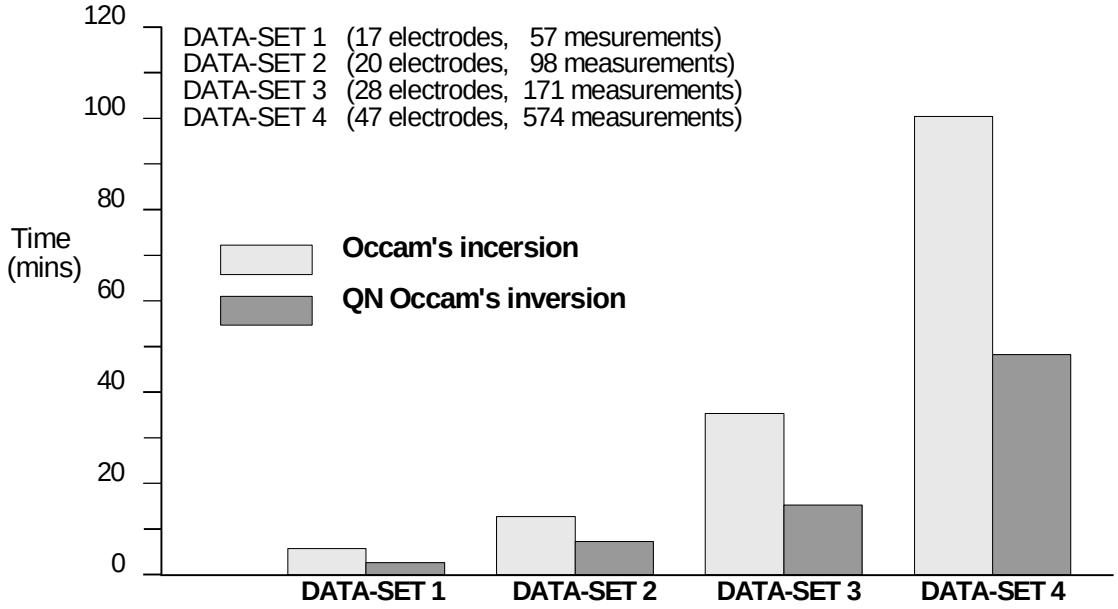

FIG. 5. Comparison of the total run-time for 4 data sets between the QN Occam and Occam inversion schemes (all tests were performed in a 486-66Mhz IMB-PC compatible).

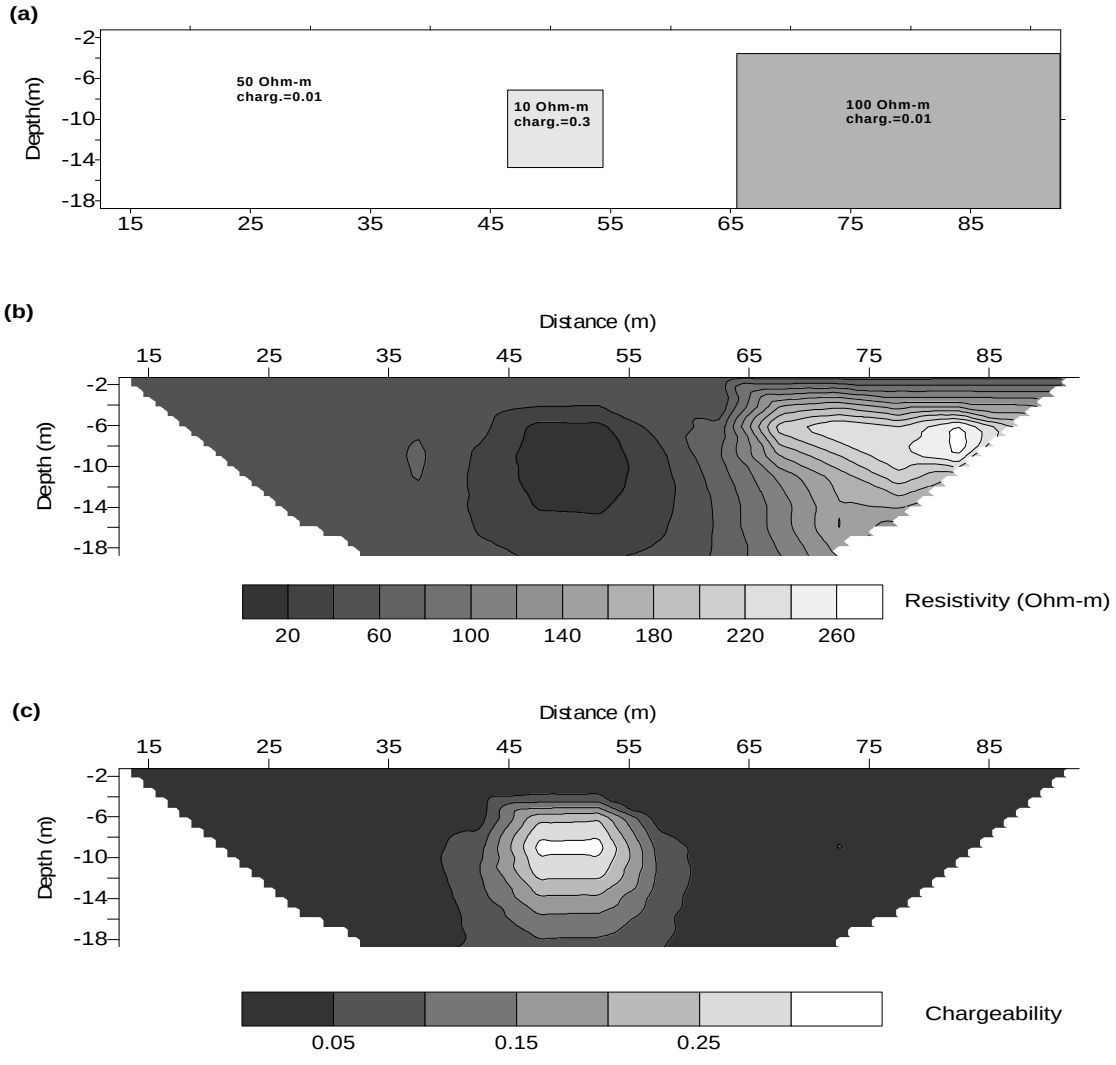

FIG. 6. Inversion of synthetic resistivity and IP dipole-dipole data (noise-free, 20 electrodes, n=8): (a) the model used to produce the synthetic data. (b)Resistivity Inversion results using the QN Occam method. (c) IP Inversion results using the QN Occam method.

the central part of the section (between 62 and 71 meters approximately which correspons to the previously known cave and another resistive anomaly (its centre is at 28 metres) which was interpreted as a new cave. A borehole was drilled and this interpretation was verified. The new cave was named ``sting'' and its position (as well as the position of the borehole) in relation to the measured section is depicted in Figure 8a.

The ``sting'' cave data were inverted using the scheme. The QN Occam inversion results after 9 iterations are depicted in Figure 8c. The RMS error for this inversion is 2.9%.This inversion was produced by adjusting the thicknesses of the parameter layers

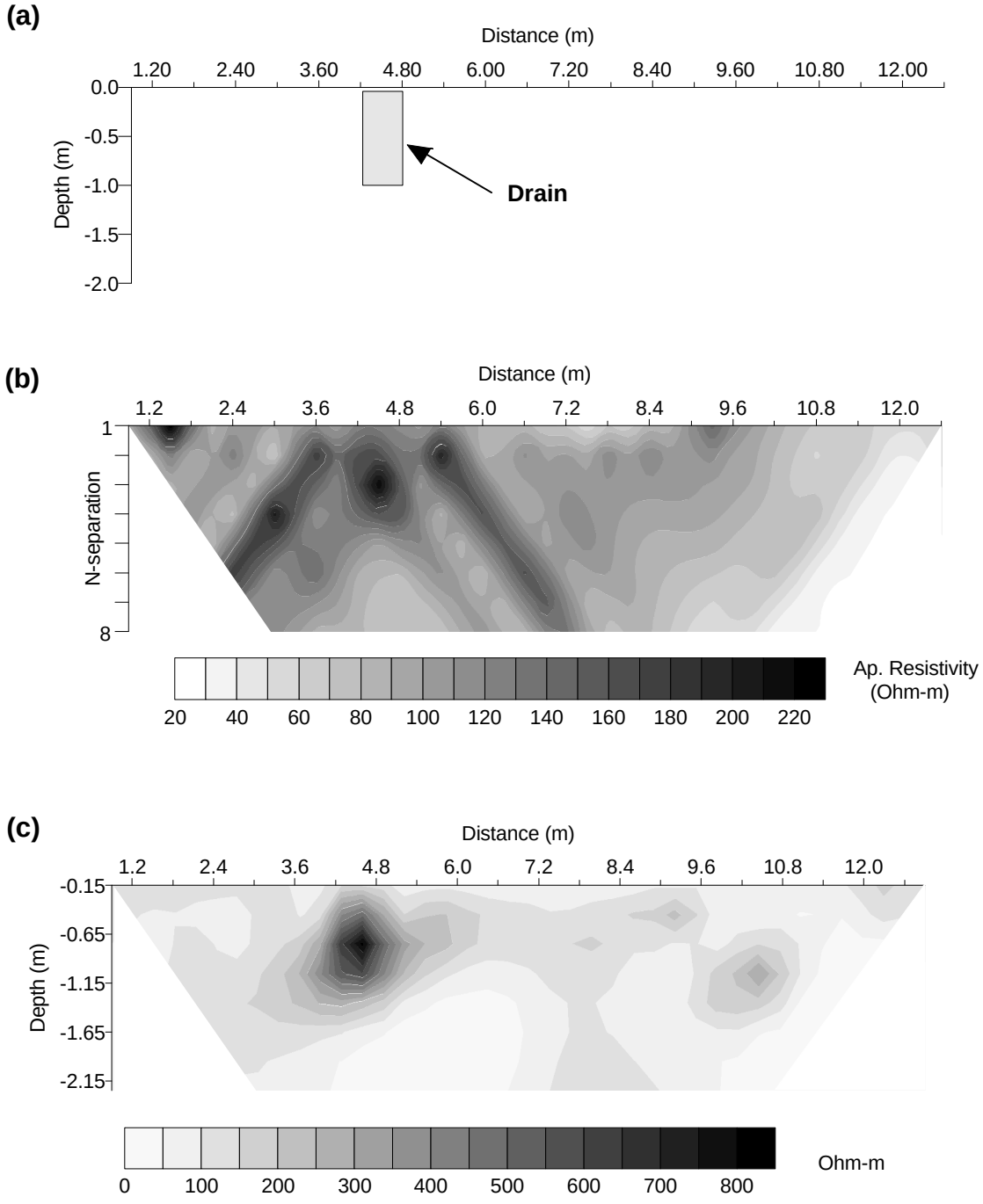

FIG. 7. Reconstruction of the dipole-dipole data measured over a drain (University of York): a) the exact location of the drain in relation to the measured section, b) the measured data set in a pseudosection form, c) reconstruction using the QN Occam algorithm (6 iterations, 7.2% RMS error).

according to the accurate *a priori* information. The inversion with the automatic parameter generation (not shown here) produced a very similar image, gave an error of 5.4% and slightly misplaced the central cave in the depth scale. This is indicative of the improvement of the data fit if the correct parameter thicknesses are chosen. In any case, several possible parameter schemes have to be tested in order to obtain the optimal solution.

The inverted image of Figure 8c delineates the two known cases fairly accurate. An artifact at the left side of the anomaly that correponds to the 'sting' cave is

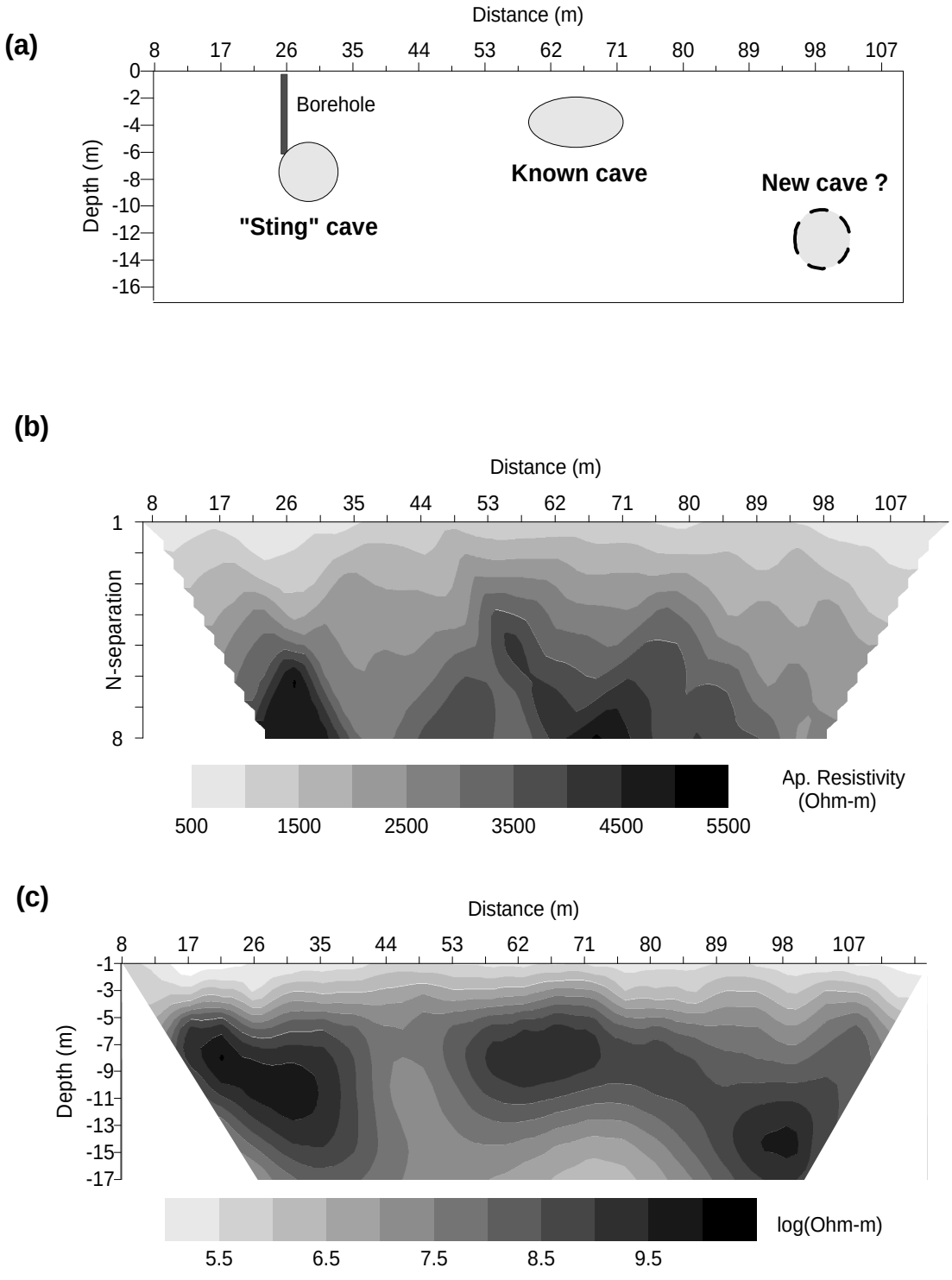

FIG. 8. Reconstruction of the dipole-dipole data measured over caves ("Sting" Cave, Williamson County, Texas): (a) the exact location of the known caves in relation to the measured section, (b) the measured data set in a pseudosection form, (c) reconstruction using the QN Occam scheme (9 iterations, 2.9% RMS error).

probably due to the fact that the measurements do not fully describe the target. Further, a pronounced resistive feature is now seen to be situated at the right-hand side of the section (centre at x=98m, z=13m). Judging by the accuracy of the reconstruction of the known caves, all reasons are satisfied to interpret the high resistive blocks as an indication of unknown cave.

CONCLUSIONS

In this work an algorithm for inverting resistivity and IP data is presented. The algorithm combines the characteristics of the smoothness constrained inversion with the computational savings that derive from using the QN Jacobian update. The conducted tests indicated that the algorithm has the following features:

- It is considerably faster than the Occam inversion for a typical size of data set. The fact that it takes a further 1-3 iterations is a more than acceptable trade-off considering the computational savings that it involves.
- In all tested cases it produced results similar to the Occam inversion and, in general, comprises all the advantages (and limitations) of the Occam inversion. These are stability, robustness to noise, and inversion with user defined characteristics.
- It is flexible since it can cope with any known resistivity array and, further, it can readily cope with ``unconventional" measuring schemes.
- Extra flexibility is achieved by allowing the incorporation of variable smoothness and, most importantly, variable parametrization.
- For all of the tested cases with real data the algorithm produced reasonably good results which do not suffer from algorithm and/or noise related artifacts.

Overall, the algorithm proved to be a reliable and useful tool for routine data interpretation and produced results which are directly appreciable by non-experts.

ACKNOWLEDGMENT

This work was performed on behalf of the research project of the Aristotle University of Thessaloniki (Greece) number 1716. The General Secretariat of Research and Technology of Greece financed the project under the framework of PENED 1995.

The authors are greatly indebted to Prof. Ahmet T. Basokur for his constructive criticism and revision of the manuscript.

REFERENCES

Broyden, C.G., 1965, A class of methods for solving nonlinear imultaneous equations: Mathematics of Computing, **19**, 577-593.

Constable, S., Parker, R., and Constable C., 1987, Occam's inversion: A practical algorithm for generating smooth models from electromagnetic sounding data: Geophysics, **52**, 289-300.

deGroot-Hedlin, C., and Constable, S., 1990, Occam's inversion to generate smooth, two-dimensional models from magnetoteluric data: Geophysics, **55**, 1613-1624.

Dahlin, T., 1993, On the automation of 2D resistivity surveying for engineering and environmental applications: Ph.D. Thesis, Lund University.

Edwards, L. S., 1977, A Modified Pseudosection for Resistivity and IP: Geophysics, **42**, 1020-1036.

Ellis, R., and Oldenburg D.W., 1994, Applied geophysical inversion: Geophys.J.Int., **116**, 5-11.

Fletcher, R., 1987, Practical methods of optimization: 2nd edition, Wiley Ltd.

Loke M.H., and Barker, R., 1996, Rapid least-squares inversion of apparent resistivity pseudosections by a quasi-Newton method: Geophysical Prospecting, **44**, 131-152.

McGillivray, P., and Oldenburg, D., 1990, Methods for calculating Frechet derivatives and sensitivities for the non-linear inverse problem: A comparative study: Geophysical Prospecting, **38**, 499-524.

Noel, M., and Walker R., 1991, Imaging archaeology by electrical resistivity tomography: a preliminary study, in Archaeological Sciences **89**, Budd, P., Chapman, B., Jackson, C. Janaway, R. and Ottaway, B., Oxbow, 295-304.

Oldenburg D., and Li Y., 1994, Inversion of induced polarization data: Geophysics, **59**, 1327-1341.

Pelton, W., Rijo, L., and Swift, J., 1978, Inversion of two-dimensional resistivity and induced polarization data: Geophysics, **43**, 788-803.

Press, W., Flannery, B., Teukolski, S., and Vetterling, W., 1987, Numerical recipes: the art of scientific computing: Cambridge University Press.

Powell, M.J.D., 1970, A hybrid method for nonlinear equations: in Numerical Methods for Nonlinear Algebraic Equations: Rabinowitz, P. (ed.), Gordon and Breach Science Bublishers, 61-74.

Sasaki, Y., 1989, 2-D joint inversion of magnetotelluric and dipole-dipole resistivity data: Geophysics, **54**, 254-262.

Sasaki, Y., 1992, Resolution of resistivity tomography inferred from numerical simulation: Geophysical Prospecting, **40**, 453-464.

Shima, H., 1990, Two-dimensional automatic resistivity inversion technique using alpha centres: Geophysics, **55**, 682-694.

Siegel,H., 1959, Mathematical formulation and type curves for induced polarization: Geophysics, **24**, 547-565.

Smith, N., and Vozoff, K., 1984, Two-dimensional DC resistivity inversion for dipole-dipole data: IEEE Trans. Geosc, **22**, 21-28.

Stretenovic, B., and Marcetic, D., 1992, Determination of the internal geometry of a land-slide using electrical tomography: Abstracts of the 54 th Meeting of the E.A.E.G., Paris, France, 1-5 June.

Tripp, A., Hohmann, G., and Swift, C., 1984, Two-dimensional resistivity inversion: Geophysics, **49**, 1708-1717.

Tsourlos P., 1995, Modelling interpretation and inversion of multielectrode resistivity survey data: Ph.D. Thesis, University of York.

Xu, B., 1993, Development of electrical resistivity imaging methods for geological and archaeological prospecting: Ph.D. Thesis, University of Durham.